

Jet transport coefficient \hat{q} in (2+1)-flavor lattice QCD

Amit Kumar,¹ Abhijit Majumder,¹ and Johannes Heinrich Weber^{2,3}

¹*Department of Physics and Astronomy, Wayne State University, Detroit, MI 48201, USA*

²*Department of Computational Mathematics, Science and Engineering & Department of Physics and Astronomy, Michigan State University, East Lansing, MI 48824, USA*

³*Institut für Physik, Humboldt-Universität zu Berlin & IRIS Adlershof, D-12489 Berlin, Germany*

(Dated: November 13, 2020)

We present the first calculation of the jet transport coefficient \hat{q} in (2+1)-flavor QCD on a 4-dimensional Euclidean lattice. Carried out in a factorized approach, the light-like propagation of a single hard parton within a jet is treated separately from the soft gluon field, off which it scatters. The mean square gain in momentum transverse to the direction of propagation is expressed in terms of the field-strength field-strength correlation function, which is then calculated on the lattice. Dispersion relations and the operator product expansion are used to relate the \hat{q} defined on the light-cone with the expectation of a diminishing series of local operators. Calculations of the local operator products are carried out at finite temperature, over a range of lattice sizes, and compared with the results from quenched calculations, perturbative and phenomenological extractions of \hat{q} .

The study of dense QCD matter, produced in relativistic heavy-ion collisions, using high transverse momentum (p_T) jets, currently boasts an almost established phenomenology [1–3]. The experimental data on various aspects of jet modification is also extensive, with high statistics available for a wide range of observables [4–14]. Almost all of the evidence points to the formation of a Quark-Gluon Plasma (QGP), a state of matter where the QCD color charge is deconfined over distances larger than the size of a proton [15, 16]. Jets are expected to undergo considerable modification within the QGP compared to confined conventional QCD matter [17].

While a lot of the theoretical development of jet quenching has been focused on modifications to the parton shower, considerably less work has been carried out on the study of the interaction between a parton in the jet with the QGP itself. Most current calculations either model the QGP as a set of slowly moving (or static) heavy scattering centers [17–20], or in terms of Hard-Thermal Loop (HTL) effective theory [21–24]. A third method assumes multiple exchanges and an effective Gaussian distribution in the 2-D momentum (transverse to the jet parton) exchange between the parton and the medium. The second moment of this distribution, averaged over events and scatterings, is referred to as \hat{q} [25]:

$$\hat{q} = \frac{\sum_{i=1}^{N_{events}} \sum_{j=0}^{N^i(L)} [k_{\perp}^{i,j}]^2}{N_{events} \times L}. \quad (1)$$

The meaning of the above equation is that given a path through a medium with a pre-determined density profile, a single parton may scatter $N^i(L)$ times while traversing a distance $L < v\tau_i$ in event i (τ_i is the lifetime of the parton which travels at a speed v). In each scattering (j), it exchanges transverse momentum $k_{\perp}^{i,j}$. In this Letter, we will only focus on momentum exchanges transverse to the direction of the jet parton, as these tend to have a dominant effect on the amount of energy lost via bremsstrahlung from the parton [20, 26].

In realistic media, created in heavy-ion collisions, the density will vary over the length L , and thus, one necessarily averages over a non-uniform profile, which could fluctuate from event to event. In most current simulations of the expanding QGP, one assumes that the density gradients are small enough over a considerable portion of the evolution that one can apply relativistic viscous fluid dynamics, which assumes local thermal equilibrium. Several successful fluid dynamical simulations, which compare to RHIC and LHC data [27, 28], have used the equation of state calculated in lattice QCD [29] as an input. Unlike the dynamical medium in a heavy-ion collision, lattice simulations assume static media in thermal equilibrium. The use of lattice QCD input in fluid-dynamical simulations is predicated on the ability to reliably coarse grain the system into space-time unit cells, over which intrinsic quantities, e.g., temperature (T), entropy density (s), pressure (P), remain approximately constant.

The calculations in this Letter are an extension of the above principle: Calculations of \hat{q} in the static medium of lattice QCD will be compared with phenomenological estimations, where jets are propagated through a QGP fluid dynamical simulation. These QGP simulations yield the space-time profiles for intrinsic quantities of the medium, e.g. $T(x, y, z, t)$, $s(x, y, z, t)$ etc. As jets are propagated through the fluid simulation, the local value of \hat{q} is obtained as $\hat{q}_0 T^3/T_0^3$, or $\hat{q}_0 s/s_0$. The fit parameter \hat{q}_0 represents the value at $T = T_0$, the maximum temperature at thermalization (s_0 is the entropy density at T_0). It is dialed to fit high p_T hadron data. In this Letter, we will compare the dimensionless ratio \hat{q}/T^3 between these different approaches [3].

Following the framework in Ref. [30], we consider a jet parton with high energy E and virtuality Q such that $E \gg Q \gg \mu_D$, the Debye mass in the medium. The choice of a large E, Q leads to a diminished coupling $\alpha_S(Q)$ with the medium, due to asymptotic freedom [31, 32]. As a result, interactions between the jet

parton and a medium of limited extent will be dominated by a single gluon exchange. In this limit, the expression for \hat{q} simplifies to the form that will be used henceforth:

$$\hat{q} = \frac{\sum_{i=1}^{N_{events}} [k_{\perp}^i]^2}{N_{events} \times L}. \quad (2)$$

In light cone coordinates, the incoming quark, traveling in the $-z$ direction, has two non-zero components, $q^+ = (q^0 + q^3)/\sqrt{2} \ll q^- = (q^0 - q^3)/\sqrt{2}$. The quark undergoes a single scattering off the gluon field in the medium and gains transverse momentum k_{\perp} (Fig. 1). In this frame, the momentum of the quark changes from,

$$q_i \equiv [q^+, q^-, 0, 0] \rightarrow q_f \equiv [q^+ + k_{\perp}^2/(2q^-), q^-, \vec{k}_{\perp}]. \quad (3)$$

The matrix element for this process is given as $\mathcal{M} = \langle q_f | \otimes \langle X | \int_0^{T_I} dt d^3x g \bar{\psi}_q(x) \gamma^{\mu} t^a A_{\mu}^a(x) \psi(x) | n \rangle \otimes | q_i \rangle$, where $|n\rangle$ and $|X\rangle$ represent the initial and final state of the medium. The factors $\psi(x)$, $\bar{\psi}(x) [= \psi^{\dagger} \gamma^0]$ and $A^a(x)$ represent the quark and gluon wave functions (and complex conjugate), with coupling g . The spatial integrations are limited within a volume $V = L^3$ and the time of interaction ranges from 0 to $T_I = L/c$ (we use particle physics units with $\hbar, c = 1$). Replacing the average over events, with an average over all initial states $|n\rangle$ (energy E_n) of the medium, weighted by a Boltzmann factor, with $\beta = 1/T$ the inverse temperature and Z the partition function of the thermal medium, we obtain,

$$\hat{q} = \sum_{n, X} \frac{e^{-\beta E_n}}{Z T_I} \int d^2 k_{\perp} k_{\perp}^2 \mathcal{M}_{n+q_i \rightarrow q_f+X}^* \mathcal{M}_{n+q_i \rightarrow q_f+X}, \quad (4)$$

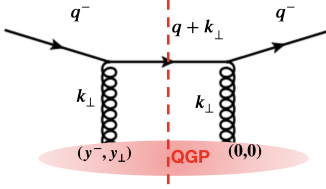


FIG. 1. A forward scattering diagram for the hard quark undergoing a single scattering off the gluon field in the plasma. The vertical dashed line represents the cut-line.

Following standard methods outlined in Ref. [30], where factors of k_{\perp} are turned into partial derivatives in y_{\perp} and y^- , we obtain the following well known expression for \hat{q} (assuming $\sum_X |X\rangle \langle X| = 1$),

$$\hat{q} = c_0 \int \frac{dy^- d^2 y_{\perp}}{(2\pi)^3} d^2 k_{\perp} e^{-i \frac{\vec{k}_{\perp}^2}{2q^-} y^- + i \vec{k}_{\perp} \cdot \vec{y}_{\perp}} \times \sum_n \langle n | \frac{e^{-\beta E_n}}{Z} g_0^2 \text{Tr}[F^{+\perp\mu}(0) F_{\perp\mu}^+(y^-, y_{\perp})] | n \rangle, \quad (5)$$

where $c_0 = 4\sqrt{2} C_R / (N_c^2 - 1)$, $C_R (= C_F$ for a quark) is the representation specific Casimir, N_c is the number of colors. In order to connect with non-perturbative calculations, we replace g with the bare coupling constant g_0

at the vertex between the hard quark and the glue field, $F^{\mu\nu} = t^a F^{a\mu\nu}$ is the bare gauge field-strength tensor.

Computing the thermal and vacuum expectation value of the non-perturbative operator $g_0^2 F^{+\perp\mu}(0) F_{\perp\mu}^+(y^-, y_{\perp})$ is challenging due to the *near* light-cone separation between the two field-strength tensors. The separation is slightly space-like $y^2 = -y_{\perp}^2 < 0$, similar to the case of a parton distribution function (PDF), as discussed in the work of Ji [33]. In that effort, one evaluates the PDF in a frame where the nucleon moves with a large momentum in the z -direction, yielding a series of covariant derivatives in $y_z \equiv y^3$. The current Letter will reach a similar conclusion, though using analytic techniques.

To recast \hat{q} in terms of a series of local operators, we apply a method of dispersion as outlined in Ref. [30]. In this approach, a generalized coefficient is defined as,

$$\hat{Q}(q^+) = c_0 \int \frac{d^4 y d^4 k e^{iky}}{(2\pi)^4} \frac{2q^- \langle g_0^2 \text{Tr}[F^{+\perp\mu}(0) F_{\perp\mu}^+(y)] \rangle}{(q+k)^2 + i\epsilon}, \quad (6)$$

where $\langle \dots \rangle \equiv \sum_n \langle n | \dots | n \rangle e^{-\beta E_n} / Z$. The object $\hat{Q}(q^+)$ has a branch cut in a region where $q^+ \sim T \ll q^-$ corresponding to the quark propagator with momentum $q+k$ going on mass shell (Fig. 1). In this region, the incoming hard quark is light-like, i.e. $q^2 = 2q^+q^- \sim 0$, and the discontinuity of $\hat{Q}(q^+)$ is related to the physical \hat{q} as

$$\left. \frac{\text{Disc}[\hat{Q}(q^+)]}{2\pi i} \right|_{\text{at } q^+ \sim T} = \hat{q}. \quad (7)$$

In addition to the thermal discontinuity, $\hat{Q}(q^+)$ also has an additional vacuum discontinuity in the region $q^+ \in (0, \infty)$ due to real hard gluon emission processes. In this region, the incoming hard quark is time-like. If instead, one takes $q^+ \ll 0$, e.g. $q^+ = -q^-$, the incoming quark becomes space-like and there is no discontinuity on the real axis of q^+ . In this deep space-like region, the quark propagator can be expanded as follows:

$$\frac{1}{(q+k)^2} \simeq \frac{-1}{2q^-(q^-(k^+ - k^-))} = \frac{-1}{2(q^-)^2} \sum_{n=0}^{\infty} \left(\frac{\sqrt{2}k_z}{q^-} \right)^n. \quad (8)$$

Using integration by parts, the factor of exchanged gluon momentum k_z [Eq. (8)] is replaced with the regular spatial derivative ∂_z acting on the field-strength $F_{\perp\mu}^+(y)$ [Eq. (6)]. A set of higher order contributions from gluon scattering diagrams can be added to promote the regular derivative to a covariant derivative (in the adjoint representation). With all factors of k removed from the integrand [Eq. (6)], except for the phase factor, k can be integrated out ($\int d^4 k e^{iky}$) to yield $\delta^4(y)$, setting y to the origin. This yields $\hat{Q}(q^+ = -q^-) \equiv \hat{Q}|_{q^+ = -q^-}$ as,

$$\hat{Q}|_{q^+ = -q^-} = c_0 \langle g_0^2 \text{Tr}[F^{+\perp\mu}(0) \sum_{n=0}^{\infty} \left(\frac{i\sqrt{2}D_z}{q^-} \right)^n F_{\perp\mu}^+(0)] \rangle / q^-. \quad (9)$$

In the above equation, each term in the series is a local gauge-invariant operator, and hence, one can directly compute their expectation value on the lattice.

To relate $\hat{Q}(q^+ = -q^-)$ to the physical \hat{q} , consider the following contour integral in the q^+ complex-plane:

$$I_1 = \oint \frac{dq^+}{2\pi i} \frac{\hat{Q}(q^+)}{(q^+ + q^-)} = \hat{Q}(q^+ = -q^-), \quad (10)$$

where the contour is taken as a small anti-clockwise circle centered around point $q^+ = -q^-$, with a radius small enough to exclude regions where $\hat{Q}(q^+)$ may have discontinuities. Alternatively, the integral can be evaluated by analytically deforming the contour over the branch cut of $\hat{Q}(q^+)$ for $q^+ \in (-T_1, \infty)$ and obtaining Eq. (10) as:

$$\hat{Q}(q^+ = -q^-) = \int_{-T_1}^{T_2} \frac{dq^+}{2\pi i} \frac{Disc[\hat{Q}(q^+)]}{(q^+ + q^-)} + \int_0^{\infty} \frac{dq^+}{2\pi i} \frac{Disc[\hat{Q}(q^+)]}{(q^+ + q^-)}. \quad (11)$$

The limits $-T_1$ and T_2 in the first integral represent lower and upper bounds of $q^+ [= k^+ + k_{\perp}^2/(2q^- + 2k^-)]$, beyond which the thermal discontinuity in $\hat{Q}(q^+)$ on the real axis of q^+ is zero. In this region, the hard incoming quark is close to on-shell, i.e. $q^2 = 2q^+q^- \approx 0$ and undergoes scattering with the medium. The second integral in Eq. (11) corresponds to the contributions from vacuum-like processes, where the time-like hard quark with momentum $q^+ \in (0, \infty)$ undergoes vacuum-like splitting. Hence, the second integral is temperature independent.

Using Eqs. (7-11), we obtain (suppressing $y^- = y_{\perp} = 0$),

$$\frac{\hat{q}}{T^3} = \frac{c_0 \sum_{n=0}^{\infty} \left(\frac{T}{q^-}\right)^{2n} \left\langle \frac{g_0^2}{T^4} \text{Tr} \left[F^{+\perp\mu} \left(\frac{i\sqrt{2}D_z}{T} \right)^{2n} F_{\perp\mu}^+ \right] \right\rangle_{(T-V)}}{(T_1 + T_2)/T}, \quad (12)$$

where the subscript T-V represents the vacuum subtracted expectation value and $T_1 + T_2 \simeq 2\sqrt{2}T$ represents a width of the thermal discontinuity of $\hat{Q}(q^+)$. The above expression of transport coefficient \hat{q} contains several features. First, each term in the series is local, allowing for their computation on the lattice. Second, the successive terms in the series are suppressed by the hard scale q^- , and hence, computing only first few terms will be sufficient [34]. We also note that the expression of \hat{q} given in Eq. (12) is applicable for the hard quark traversing either the pure glue plasma or a quark-gluon plasma.

To compute the operators on the lattice, we perform the Wick rotation $x^0 \rightarrow -ix^4, A^0 \rightarrow iA^4 \implies F^{0i} \rightarrow iF^{4i}$. We study the first three non-zero operators in the \hat{q} series [35], $\hat{O}_n = g_0^2/T^4 \sum_{i=1}^2 \text{Tr}(F^{3i}[i\sqrt{2}D_z/T]^{2n}F^{3i}) - [3 \rightarrow 4]$, and discretize $g_0 F_{\mu\nu}$ via tadpole-improved clover-leaf operators projected to anti-Hermitian traceless matrices,

$$ig_0 \mathcal{F}_{\mu\nu}(x) = \frac{\mathcal{P}Q_{\mu\nu}(x)}{a_L^2 u_0^4} = ig_0 F_{\mu\nu} + \mathcal{O}(a_L^2) \quad (13)$$

with $Q_{\mu\nu} = [U_{\mu,\nu} + U_{\nu,-\mu} + U_{-\mu,-\nu} + U_{-\nu,\mu}]/4$ ($U_{\mu,\nu}$ being the plaquette) and $\mathcal{P}Q = (Q - Q^\dagger - \text{Tr}[Q - Q^\dagger]/N_c)/2$. We

define $u_0 = \sqrt[4]{\langle \text{Tr}[U_{\mu,\nu}] \rangle / N_c}$ and use symmetric, tadpole-improved differences in covariant derivatives. Note that each operator contains temperature-independent, additive contributions that diverge in the continuum limit, but cancel exactly in the vacuum-subtracted operators.

We generate $T > 0$ lattices with aspect ratio $n_\sigma/n_\tau = 4$ for $n_\tau = 4, 6$ and 8 [$T = 1/(a_L n_\tau)$], and also corresponding $T = 0$ lattices with $n_\tau = n_\sigma$ using the MILC code [36] and the USQCD software stack [37]. We use the Rational Hybrid Monte Carlo (RHMC) algorithm [38] with highly improved staggered quark (HISQ) action [39] and tree-level Symanzik gauge action [40, 41] for (2+1)-flavor QCD. The leading cutoff effects are $\mathcal{O}(a^4)$ and $\mathcal{O}(g_0^2 a^2)$. We employ tuned input parameters (bare lattice coupling $\beta_0 = 10/g_0^2$, and bare quark masses), and use the r_1 lattice scale following Refs. [40–43] by the HotQCD and TUMQCD collaborations. This setup has a physical strange and two degenerate light quarks with $m_l = m_s/20$ corresponding to a pion mass of about 160 MeV in the continuum limit. We generate pure gauge ensembles via the heat-bath algorithm using Wilson gauge action [44] with $\beta_0 = 6/g_0^2$ and leading cutoff effects $\mathcal{O}(a^2)$. See Supplemental Material for details about the gauge ensembles [45].

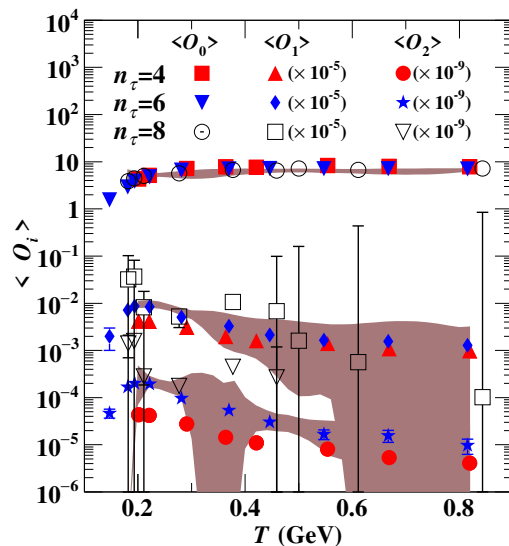


FIG. 2. T and n_τ dependence of the expectation values of vacuum-subtracted operators \hat{O}_n in (2+1)-flavor QCD. The features are qualitatively similar in SU(3) pure gauge theory. The bands represent continuum estimates.

Our data set does not show unambiguous linear scaling towards the continuum due to lack of fine enough lattices (three ensembles with $n_\tau \geq 8$ would be necessary) and insufficient statistics for $n_\tau = 8$, especially in \hat{O}_1, \hat{O}_2 . In order to provide a continuum estimate [46], we first interpolate for each n_τ the expectation value of \hat{O}_n in the temperature using splines and propagate the errors via bootstrap. Then we extrapolate linearly to the

continuum at fixed temperature by varying the subset of n_τ values and use either zero, one, or two monomials in $1/n_\tau^2$. If we cannot propagate the error directly, we resort to bootstrap for the error propagation. Finally, we estimate the continuum limit as the average of all fits and a corrected error from the spread of the fits if the latter exceeds the naively propagated error.

The vacuum-subtracted expectation values of the first three non-zero operators \hat{O}_n , $n = 0, 1, 2$, computed in (2+1)-flavor QCD over a range of temperatures covering $150\text{MeV} < T < 850\text{MeV}$, are presented in Fig. 2 for $n_\tau = 8, 6$ and 4 [47]. The results in SU(3) pure gauge theory are qualitatively similar. Although the \hat{O}_n , $n \geq 1$ appear to be sharply peaked at temperatures slightly above the corresponding transition region, namely at $T \approx 220$ MeV in (2+1)-flavor QCD or at $T \approx 300$ MeV in the SU(3) pure gauge theory, their impact on \hat{q} is negligible at the achievable accuracy. This can be understood from the fact that the \hat{O}_n are suppressed in Eq. (12) by powers of the ratio $(T/q^-)^{2n}$ compared to the leading term \hat{O}_0 .

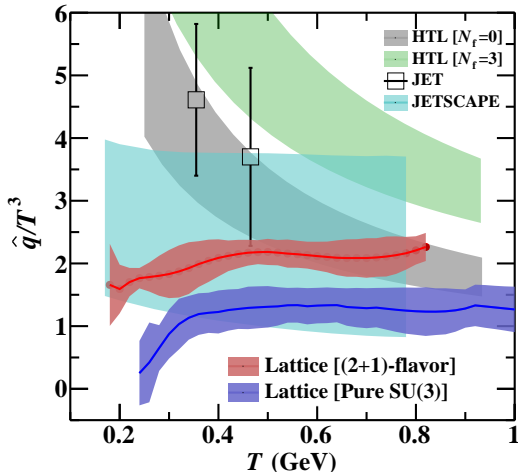


FIG. 3. Lattice QCD determination of \hat{q} for a 100 GeV quark traversing a pure glue and (2+1)-flavor QCD plasma. Continuum results are estimated using $n_\tau = 8, 6$ and 4. Also plotted are the phenomenological extractions from the JET [3] and JETSCAPE [48] collaborations, and LO-HTL calculations from Ref. [49] with $\alpha_S(\mu^2)$ evaluated at $2\pi T \leq \mu \leq 4\pi T$.

Given the one gluon exchange approximation [Eq. (9)], the q^- dependence of \hat{q}/T^3 is indeed small. In the following, the light-cone momentum q^- of the hard quark traversing the plasma was taken to be 100 GeV. The temperature dependence of the resulting \hat{q}/T^3 is shown in Fig. 3 for the continuum estimates using both the quenched SU(3) or unquenched (2+1)-flavor lattices. The red band represents \hat{q}/T^3 for (2+1)-flavor QCD (HISQ and Symanzik gauge action) and constrains $\hat{q}/T^3 = 2.21(23)$ at $T = 800$ MeV. The blue band represents \hat{q}/T^3 as a function of T for SU(3) pure gluon plasma (Wilson gauge action) and constrains $\hat{q}/T^3 = 1.24(37)$ at $T = 800$

MeV. Errors in both results are large due to the challenges in the continuum extrapolation.

The transport coefficient \hat{q}/T^3 exhibits a rapid rise in magnitude in the transition region and slightly above, i.e. in the temperature range $150\text{MeV} \lesssim T \lesssim 250\text{MeV}$ for (2+1)-flavor QCD or $250\text{MeV} \lesssim T \lesssim 350\text{MeV}$ for the SU(3) pure gauge theory, and is flat within errors above 400 MeV. This is similar to the T dependence of the scaled entropy density s/T^3 [50]. The reduced magnitude of the upward shift of the (2+1)-flavor QCD \hat{q}/T^3 calculations can be understood by scaling the additional quark degrees of freedom with the ratio of quark-to-gluon Casimir [$C_F/C_A = (N_c^2 - 1)/(2N_c^2) = 4/9$]. Expectedly, the lattice results do not show any log-like rise at lower T , as one observes in any leading order (LO) perturbative HTL based calculation [51] (Note the HTL bands in Fig. 3).

In Fig. 3, we also present a comparison with phenomenological extractions of \hat{q}/T^3 extracted by the JET [3] and JETSCAPE [48] collaborations. The JET collaboration applied several disparate models of energy loss with either a sole T dependence of the ratio \hat{q}/T^3 , or one obtained from HTL effective theory [52]. The JETSCAPE extraction applied an amalgam of theories for different epochs of the jet shower, with a data-driven (Bayesian) determination of \hat{q}/T^3 , allowed to depend on T , the energy and scale of a given parton in the shower.

In this Letter, we carried out the first semi-realistic (2+1)-flavor lattice QCD calculation of the jet quenching parameter \hat{q} , which is the leading coefficient affecting jet modification in the QGP. This represents a rigorous *first-principles* framework for calculations of \hat{q} . Continuum estimates were presented for the SU(3) pure gluon plasma and (2+1)-flavor QCD. While the proximity of the lattice calculations with phenomenological extractions is encouraging, several caveats need to be considered: The perturbative portions of the current calculation will have to be extended to higher-order, at which point \hat{q} will have to be renormalized (including possible operator mixing). The \hat{q} used in the JET and JETSCAPE extraction (carried out in the single gluon approximation) are similarly not renormalized (the JETSCAPE extractions allow for E, μ dependence but no operator mixing). Improved comparisons in the future will require rigorous control of the continuum extrapolation through the use of finer lattices and higher statistics. The current lattice calculation included a single parton undergoing a single scattering off the medium simulated on the lattice. Future efforts will need to consider the effect of gluon emission and multiple interactions within the lattice, and the matching of the renormalized lattice results to a continuum scheme, e.g., \overline{MS} [53]. Phenomenological extractions will also need to be performed with a renormalized \hat{q} in the same scheme.

Acknowledgements. This work was supported in part by the National Science Foundation (NSF) under grant number ACI-1550300 (SSI-JETSCAPE), by the U.S. Department of Energy (DOE) under grant number DE-

SC0013460. JHW's research is funded by the Deutsche Forschungsgemeinschaft (DFG, German Research Foundation) - Projektnummer 417533893/GRK2575 "Re-thinking Quantum Field Theory".

-
- [1] A. Majumder and M. Van Leeuwen, *Prog. Part. Nucl. Phys.* **66**, 41 (2011), arXiv:1002.2206 [hep-ph].
- [2] S. Cao and X.-N. Wang, (2020), arXiv:2002.04028 [hep-ph].
- [3] K. M. Burke *et al.* (JET Collaboration), *Phys. Rev.* **C90**, 014909 (2014), arXiv:1312.5003 [nucl-th].
- [4] S. S. Adler *et al.* (PHENIX), *Phys. Rev.* **C76**, 034904 (2007), arXiv:nucl-ex/0611007.
- [5] A. Adare *et al.* (PHENIX), *Phys. Rev. Lett.* **105**, 142301 (2010), arXiv:1006.3740 [nucl-ex].
- [6] J. Adams *et al.* (Star), *Phys. Rev.* **C75**, 034901 (2007), nucl-ex/0607003.
- [7] C. Adler *et al.* (STAR), *Phys. Rev. Lett.* **90**, 082302 (2003), nucl-ex/0210033.
- [8] S. Chatrchyan *et al.* (CMS), *Phys. Rev. Lett.* **113**, 132301 (2014), [Erratum: *Phys. Rev. Lett.* 115, no. 2, 029903 (2015)], arXiv:1312.4198 [nucl-ex].
- [9] S. Acharya *et al.* (ALICE), *Phys. Lett.* **B776**, 249 (2018), arXiv:1702.00804 [nucl-ex].
- [10] B. A. Cole (ATLAS Collaboration), *J.Phys.* **G38**, 124021 (2011).
- [11] B. Abelev *et al.* (ALICE), *JHEP* **03**, 013 (2014), arXiv:1311.0633 [nucl-ex].
- [12] S. Chatrchyan *et al.* (CMS), *Phys. Rev.* **C90**, 024908 (2014), arXiv:1406.0932 [nucl-ex].
- [13] CMS-PAS-HIN-11-004 925220, (2011).
- [14] G. Aad *et al.* (ATLAS), *Phys. Rev. Lett.* **114**, 072302 (2015), arXiv:1411.2357 [hep-ex].
- [15] E. V. Shuryak, *Phys. Rept.* **61**, 71 (1980).
- [16] E. V. Shuryak, *Phys. Lett.* **B78**, 150 (1978).
- [17] M. Gyulassy and X.-N. Wang, *Nucl. Phys.* **B420**, 583 (1994), nucl-th/9306003.
- [18] R. Baier, Y. L. Dokshitzer, S. Peigne, and D. Schiff, *Phys. Lett.* **B345**, 277 (1995), arXiv:hep-ph/9411409.
- [19] X.-N. Wang, M. Gyulassy, and M. Plumer, *Phys. Rev.* **D51**, 3436 (1995), arXiv:hep-ph/9408344.
- [20] R. Baier, Y. L. Dokshitzer, A. H. Mueller, S. Peigne, and D. Schiff, *Nucl. Phys.* **B484**, 265 (1997), hep-ph/9608322.
- [21] J. Frenkel and J. C. Taylor, *Nucl. Phys.* **B334**, 199 (1990).
- [22] E. Braaten and R. D. Pisarski, *Phys. Rev. Lett.* **64**, 1338 (1990).
- [23] E. Braaten and R. D. Pisarski, *Nucl.Phys.* **B337**, 569 (1990).
- [24] P. Arnold, G. D. Moore, and L. G. Yaffe, *JHEP* **06**, 030 (2002), hep-ph/0204343.
- [25] R. Baier, *Nucl. Phys.* **A715**, 209 (2003), arXiv:hep-ph/0209038.
- [26] R. Baier, Y. L. Dokshitzer, A. H. Mueller, S. Peigne, and D. Schiff, *Nucl. Phys.* **B483**, 291 (1997), hep-ph/9607355.
- [27] H. Song, S. A. Bass, U. Heinz, T. Hirano, and C. Shen, *Phys. Rev. Lett.* **106**, 192301 (2011), [Erratum: *Phys. Rev. Lett.* 109, 139904 (2012)], arXiv:1011.2783 [nucl-th].
- [28] C. Shen, U. Heinz, P. Huovinen, and H. Song, *Phys. Rev.* **C84**, 044903 (2011), arXiv:1105.3226 [nucl-th].
- [29] P. Huovinen and P. Petreczky, *Nucl. Phys.* **A837**, 26 (2010), arXiv:0912.2541 [hep-ph].
- [30] A. Majumder, *Phys. Rev.* **C87**, 034905 (2013).
- [31] H. D. Politzer, *Phys. Rev. Lett.* **30**, 1346 (1973).
- [32] D. J. Gross and F. Wilczek, *Phys. Rev. Lett.* **30**, 1343 (1973).
- [33] X. Ji, *Phys. Rev. Lett.* **110**, 262002 (2013), arXiv:1305.1539 [hep-ph].
- [34] The derivative in the z -direction includes contributions from momenta up to $k_z = \pi/a_L$. Accordingly, the size and necessary number of the extra terms increases for finer lattice spacings, and the calculation has to be restricted to lattices spacings that satisfy $(a_L q^-)^2 \gg 2\pi^2$.
- [35] Operators with odd powers of the covariant derivative in Eq. (12) are odd under parity, and thus their expectation value vanishes on ensembles generated with an action that is invariant under parity. Operators mixing magnetic and electric field strengths that are included in Eq. (12) vanish on ensembles with trivial topology.
- [36] MILC collaboration code for lattice QCD calculations, public version on GitHub, <https://github.com/milc-qcd/milc-qcd/>; <http://www.physics.utah.edu/~detar/milc/milcv7.html> (2017).
- [37] SciDAC software modules for optimization: QDP-1.11.1, QIO-2.5.0, QLA-1.9.0, QMP-2.5.1, QOPQDP-0.21.1; <https://www.usqcd.org/usqcd-software/>.
- [38] M. Clark, A. Kennedy, and Z. Sroczynski, *Nucl. Phys. B Proc. Suppl.* **140**, 835 (2005), arXiv:hep-lat/0409133.
- [39] E. Follana, Q. Mason, C. Davies, K. Hornbostel, G. P. Lepage, J. Shigemitsu, H. Trotter, and K. Wong, *Physical Review D* **75** (2007), 10.1103/physrevd.75.054502.
- [40] A. Bazavov *et al.* (HotQCD), *Phys. Rev. D* **90**, 094503 (2014), arXiv:1407.6387 [hep-lat].
- [41] A. Bazavov, N. Brambilla, P. Petreczky, A. Vairo, and J. H. Weber (TUMQCD), *Phys. Rev. D* **98**, 054511 (2018), arXiv:1804.10600 [hep-lat].
- [42] A. Bazavov, N. Brambilla, H. T. Ding, P. Petreczky, H. P. Schadler, A. Vairo, and J. Weber, *Phys. Rev. D* **93**, 114502 (2016), arXiv:1603.06637 [hep-lat].
- [43] A. Bazavov, P. Petreczky, and J. Weber, *Phys. Rev. D* **97**, 014510 (2018), arXiv:1710.05024 [hep-lat].
- [44] K. G. Wilson, *Phys. Rev.* **D10**, 2445 (1974).
- [45] See Supplemental Material for details about parameter settings used in generating gauge ensembles..
- [46] It is known that $\mathcal{O}(a^4)$ cutoff effects are non-negligible for the QCD ensembles at $n_\tau \leq 6$ [41, 43]. For this reason, our data set is insufficient for a genuine continuum extrapolation with fully-controlled error propagation.
- [47] A. Kumar, A. Majumder, and J. H. Weber, in *10th International Conference on Hard and Electromagnetic Probes of High-Energy Nuclear Collisions: Hard Probes 2020* (2020) arXiv:2009.05655 [nucl-th].
- [48] R. Soltz (Jetscape), *PoS HardProbes2018*, 048 (2019).
- [49] Y. He, T. Luo, X.-N. Wang, and Y. Zhu, *Phys. Rev.* **C91**, 054908 (2015), [Erratum: *Phys. Rev.* C97, no. 1, 019902 (2018)], arXiv:1503.03313 [nucl-th].
- [50] O. Philipsen, *Prog. Part. Nucl. Phys.* **70**, 55 (2013), arXiv:1207.5999 [hep-lat].
- [51] G.-Y. Qin and A. Majumder, *Phys.Rev.Lett.* **105**, 262301 (2010), arXiv:0910.3016 [hep-ph].

- [52] S. Caron-Huot, *Phys. Rev. D* **79**, 065039 (2009), [arXiv:0811.1603 \[hep-ph\]](#).
- [53] S. Capitani, *Phys. Rept.* **382**, 113 (2003), [arXiv:hep-lat/0211036 \[hep-lat\]](#).
- [54] A. Hasenfratz and P. Hasenfratz, , 241 (1980).
- [55] S. Booth *et al.* (QCDSF-UKQCD), *Phys. Lett. B* **519**, 229 (2001), [arXiv:hep-lat/0103023](#).
- [56] A. Deur, S. J. Brodsky, and G. F. de Tera mond, *Progress in Particle and Nuclear Physics* **90**, 1–74 (2016).

Supplemental Material for “Jet transport coefficient \hat{q} in (2+1)-flavor lattice QCD”

In this document, we list the parameters used in generating gauge ensembles for pure SU(3) and (2+1)-flavor QCD lattices. In the presented lattice calculations, the unquenched lattices were generated at the physical value of the strange quark mass m_s and the light sea quark masses of $m_l = m_s/20$ using the HISQ and tree-level Symanzik improved gauge action. We employed the Rational Hybrid Monte Carlo algorithm (RHMC). In Table I, II and III, we present the strange quark mass (am_s) in units of lattice spacing a , temperature (T) and time units (TU) for $n_\tau = 4, 6, 8$ and their vacuum analog $T = 0$. The temperatures for different $\beta_0 = 10/g_0^2$'s have been fixed using the r_1 scale and taken from Refs. [41].

$\beta_0 = 10/g_0^2$	am_s	T (MeV)	#TUs($T \neq 0$)	#TUs($T=0$)
5.9	0.132	201	10000	10000
6.0	0.1138	221	10000	10000
6.285	0.079	291	10000	10000
6.515	0.0603	364	10000	10000
6.664	0.0514	421	20000	10000
6.95	0.0386	554	10000	10000
7.15	0.032	669	10000	10000
7.373	0.025	819	10000	10000

TABLE I. The parameters to generate (2+1)-flavor QCD gauge ensembles with $m_l = m_s/20$ for lattice size $n_\tau = 4$ with aspect ratio $n_s/n_\tau = 4$.

$\beta_0 = 10/g_0^2$	am_s	T (MeV)	#TUs($T \neq 0$)	#TUs($T=0$)
6.0	0.1138	147	10000	10000
6.215	0.0862	181	10000	10000
6.285	0.079	194	10000	10000
6.423	0.067	222	7600	10000
6.664	0.0514	281	10000	7000
6.95	0.0386	370	10000	8000
7.15	0.032	446	10000	8600
7.373	0.025	547	10000	10000
7.596	0.0202	667	8600	10000
7.825	0.0164	815	9140	10000

TABLE II. The parameters to generate (2+1)-flavor QCD gauge ensembles with $m_l = m_s/20$ for lattice size $n_\tau = 6$ with aspect ratio $n_s/n_\tau = 4$.

In Table IV, V and VI, we provide β_0 , temperature and the collected statistics for pure SU(3) lattices. The scale setting was done using the two-loop perturbative renormalization group (RG) equation with non-perturbative correction factor [$f(\beta_0)$] given as

$$a = \frac{f(\beta_0)}{\Lambda_L} \left[\frac{11g_0^2}{16\pi^2} \right]^{\frac{-51}{121}} \exp \left[\frac{-8\pi^2}{11g_0^2} \right] \quad (1)$$

where Λ_L is a lattice parameter. We estimated the non-perturbative factor by adjusting the function $f(\beta_0)$ such that T_c/Λ_L is independent of bare coupling constant g_0 . In this calculation, the Λ_L was set 5.5 MeV [54–56] and the critical temperature to $T_c \approx 265$ MeV [50].

$\beta_0 = 10/g_0^2$	am_s	T (MeV)	#TUs($T \neq 0$)	#TUs($T=0$)
6.515	0.0604	182	7300	6400
6.575	0.0564	193	8650	6800
6.664	0.0514	211	10000	5000
6.95	0.0386	277	10000	5950
7.28	0.0284	377	10000	6550
7.5	0.0222	459	10000	5000
7.596	0.0202	500	10000	9400
7.825	0.0164	611	10000	7900
8.2	0.01167	843	10000	5000

TABLE III. The parameters to generate (2+1)-flavor QCD gauge ensembles with $m_l = m_s/20$ for lattice size $n_\tau = 8$ with aspect ratio $n_s/n_\tau = 4$.

$\beta_0 = 6/g_0^2$	T (MeV)	#TUs($T \neq 0$)	#TUs($T=0$)
5.6	209	10000	10000
5.7	271	10000	10000
5.8	336	10000	10000
5.9	406	10000	10000
6.0	482	10000	10000
6.2	658	10000	10000
6.35	816	10000	10000
6.5	1003	10000	10000
6.6	1146	10000	10000

TABLE IV. The parameters to generate pure SU(3) gauge ensembles using Wilson’s pure SU(3) gauge action for lattice size $n_\tau = 4$ with aspect ratio $n_s/n_\tau = 4$.

$\beta_0 = 6/g_0^2$	T (MeV)	#TUs($T \neq 0$)	#TUs($T=0$)
5.60	139	10000	10000
5.85	247	10000	10000
5.90	271	10000	10000
6.00	321	10000	10000
6.10	377	10000	10000
6.25	472	10000	10000
6.45	625	10000	10000
6.60	764	10000	10000
6.75	929	10000	10000
6.85	1056	10000	10000

TABLE V. The parameters to generate pure SU(3) gauge ensembles using Wilson’s pure SU(3) gauge action for lattice size $n_\tau = 6$ with aspect ratio $n_s/n_\tau = 4$.

$\beta_0 = 6/g_0^2$	T (MeV)	#TUs($T \neq 0$)	#TUs($T=0$)
5.70	135	10000	10000
5.95	221	10000	10000
6.00	241	10000	10000
6.10	283	10000	10000
6.20	329	10000	10000
6.35	408	10000	10000
6.55	536	10000	10000
6.70	653	10000	10000
6.85	792	10000	10000
6.95	899	10000	10000

TABLE VI. The parameters to generate pure SU(3) gauge ensembles using Wilson's pure SU(3) gauge action for lattice size $n_\tau = 8$ with aspect ratio $n_s/n_\tau = 4$.